Decomposition in as-grown (Ga,In)(N,As) quantum wells

X. Kong[a] and A. Trampert
Paul-Drude-Institut für Festkörperelektronik, Hausvogteiplatz 5–7, D-10117 Berlin, Germany

E. Tournié
Université Montpellier II-Centre d'Electronique et de Micro-optoélectronique de Montpellier (CEM2), Unité Mixte de Recherche (UMR) Centre National de la Recherche Scientifique (CNRS) 5507, Place Eugène Bataillon, F-34095 Montpellier, France

K. H. Ploog
Paul-Drude-Institut für Festkörperelektronik, Hausvogteiplatz 5–7, D-10117 Berlin, Germany

(Received 25 April 2005; accepted 24 August 2005; published online 17 October 2005)

We report on the investigation of the local element distribution in as-grown (Ga,In)(N,As) quantum wells with high In and N contents by using low-loss electron energy-loss spectroscopy combined with dark-field transmission electron microscopy. The (Ga,In)(N,As) quantum wells were grown on GaAs(001) substrates at different growth temperatures by molecular-beam epitaxy. Lateral modulations on the nanometer scale were detected with reversal In and N distributions pointing to the existence of regions with a more favorable Ga–N and In–As bond configurations, respectively. These composition fluctuations are the driving force for the morphological instabilities at the interfaces. Lowering the growth temperature of the quantum well results in a more homogeneous element distribution of the quaternary compound. This result is discussed with regard to the influence of the epitaxial strain and cohesive bond energy on the alloy formation during epitaxial growth. © *2005 American Institute of Physics*. [DOI: 10.1063/1.2108108]

The dilute (Ga,In)(N,As) nitrides have been suggested as an attractive semiconductor material system for realizing GaAs-based laser diodes operating in the 1.3–1.55 μm optical fiber window.[1] However, when incorporating more than 2% N and 25% In that are required for reaching the desired wavelength range, the structural quality of the resultant (Ga,In)(N,As) quantum wells (QWs) deteriorates due to the large miscibility gap and the phase separation tendency.[2,3] As a consequence, composition fluctuations and interface undulations are generally developed that can only be avoided by the growth at low temperatures yielding, however, a low photoluminescence (PL) efficiency.[4] The postgrowth annealing improves the PL efficiency again but results in the undesired blueshift of the emission wavelength.[5] Presently, most investigations on the microstructure emphasize the change in the atomic configuration between as-grown and annealed samples demonstrating an increase of In–N bonds after annealing. This fact is considered to be responsible for the blueshift of the PL line.[6] However, the origin of the interface roughness as well as the correlation between growth morphology and resultant microstructure of (Ga,In)(N,As) QWs have not been considered in detail so far. In fact, the growth morphology and composition fluctuation of as-grown QWs have a great influence on the efficiency of the postgrowth annealing process[7–9] and, in general, on the optical properties of the complete laser structure.

In this letter, we investigate the In and N distribution of as-grown (Ga,In)(N,As) QWs by transmission electron microscopy (TEM) and electron energy-loss (EEL) spectroscopy, which are powerful techniques for probing the chemical composition and electronic structure of III-V semiconductors with high spatial resolution.[10–12] In the first part of the letter, the experimental method is described that is used to analyze the local In and N concentration from low-loss EEL spectra. In the second part, we present its application on quaternary (Ga,In)(N,As) QW structures embedded in GaAs layers. Lateral fluctuations of the In and N concentration along the QWs are observed indicating a favorable Ga–N and In–As configuration, respectively, in spite of a higher resultant local strain.

The (Ga,In)(N,As) QWs were grown on GaAs (001) substrates in a molecular-beam epitaxy system equipped with conventional sources for the group-III elements as well as the As element, and with a rf-plasma source for the N. For each sample, firstly a GaAs buffer layer was grown at about 580 °C. The growth temperature was then decreased to 400–430 °C for growing the $Ga_{1-x}In_xN_yAs_{1-y}$ QWs of about 10 nm thickness and a GaAs layer of about 3 nm. The remaining GaAs top barrier layer (~65 nm) was then grown at 580 °C again.[13] The cross-sectional TEM specimens used for the EEL spectroscopy analysis were prepared by the conventional mechanical grinding and dimpling followed by ion-beam thinning at room temperature in a Gatan precision ion polishing system. The samples were investigated in a JEOL microscope with LaB_6 cathode operating at 300 kV. This microscope is equipped with a post-column Gatan Enfina EEL spectrometer. The energy resolution is about 1.5 eV according to the full width at half maximum (FWHM) of the zero-loss peak. During the EEL spectroscopy, the QWs were oriented parallel to the incident electron beam in such a way that the spectra taken from the QWs were not affected by overlapping GaAs regions. Typical collection times for each spectrum were about 1 s in order to decrease the influence of irradiation damage and hydrocarbon contamination. All spectra were collected in the diffraction mode with a semiangle of about 3.5 mrad and were corrected for dark current and gain variations within the spectrometer. The standard Fourier-log deconvolution technique was applied to remove

[a]Electronic mail: xkong@pdi-berlin.de

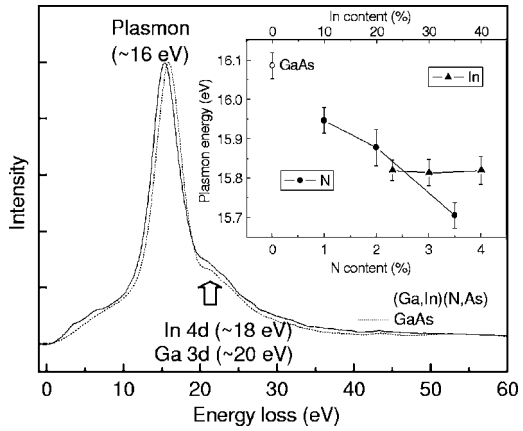

FIG. 1. The low-loss EEL spectra from GaAs and (Ga,In)(N,As). Inset shows the experimental plasmon energies vs N and In contents.

multiple inelastic scattering including the multiple plasmon excitations.[14] The Kramers-Kronig analysis was utilized to remove the plasmon excitation and to get the imaginary part $\varepsilon_2(E)$ of the dielectric function.

Figure 1 shows EEL spectra from GaAs and (Ga, In)(N,As) in the low-loss region reflecting two main characteristics: the plasmon excitation at about 16 eV and the broad peak including the In 4*d* (above 18 eV) and the Ga 3*d* (above 20 eV) interband transitions, which are superimposed on the rapidly falling tail of the plasmon excitation.[12] Both features are utilized to quantitatively measure the N, Ga, and In contents independently and simultaneously from one low-loss spectrum, as demonstrated in the following. The In and Ga mole fractions of the (Ga,In)(N,As) alloy were analyzed from the integration of the In 4*d* and Ga 3*d* transition intensities in the ε_2 spectrum, in which the influence of the plasmon peak has been removed allowing a better background fit with an inverse power law. For this purpose, the Ga and In differential cross sections were experimentally determined from the GaAs substrate and from reference samples with known In and Ga contents, respectively. The corresponding Ga contribution is analyzed by applying the same method when separating overlapping edges in the EEL spectra.[15–17] Then, the ratio between the Ga and In cross sections in the integration range (18–40 eV) before the As $M_{4,5}$ edge (~42 eV) was calculated and used to isolate the pure Ga 3*d* transition. This allows to measure the Ga concentration by normalizing to 100% Ga in the GaAs substrate. Finally, the In concentration was determined by the simple relation $\mathrm{In}:\mathrm{Ga}=x:(1-x)$ applicable for these quaternary alloys.[18]

On the other hand, the plasmon excitation corresponds to the collective oscillations of valence electrons, and its energy E_p strongly depends on the effective electron mass.[14] Therefore, the shift of E_p is correlated to the change of the band structure and thus to the change of the chemical composition of the compound semiconductor. In order to verify this dependency for $Ga_{1-x}In_xN_yAs_{1-y}$, the plasmon energies were experimentally determined for two sets of reference samples containing three QWs with systematic variations of In and N concentrations, respectively. The three QWs in the first sample contain a constant N (2.5%) but increasing In content (23%, 30%, and 40%), whereas the QWs in the second reference sample consists of a fixed In (35%) and variable N content (1%, 2%, and 3.5%). The weak contrast variation in the chemically sensitive (002) dark-field images of the reference samples indicates the small composition fluctuation along the QWs. The average plasmon energies and their standard variations calculated from ten EEL spectra along every QW in the two reference samples are summarized in the inset of Fig. 1. The results demonstrate that, within the composition range of interest, E_p is sensitively depending on the N content but is almost independent on the In content.[19] This conclusion is in agreement with theoretical and experimental results, which demonstrate a stronger bowing effect on the band structure for the incorporation of N compared to In atoms.[20] Therefore, the N concentration can directly be determined according to the shift of E_p relative to its position for the GaAs substrate.

Based on this low-loss EEL spectroscopy method, we have investigated the origin of the morphological instabilities and contrast modulations detected in as-grown (Ga,In)(N,As) QWs. For this purpose, we have compared two samples, which contain QWs with nominally identical compositions of about 3% N and 30% In, which are however, grown at slightly different temperatures. For the QW grown at 430 °C, the cross-sectional (002) dark-field TEM image in Fig. 2(a) reveals strong interface undulations and contrast modulations along the QW pointing to large composition fluctuations, whereas the QW grown at 410 °C [Fig. 2(c)]

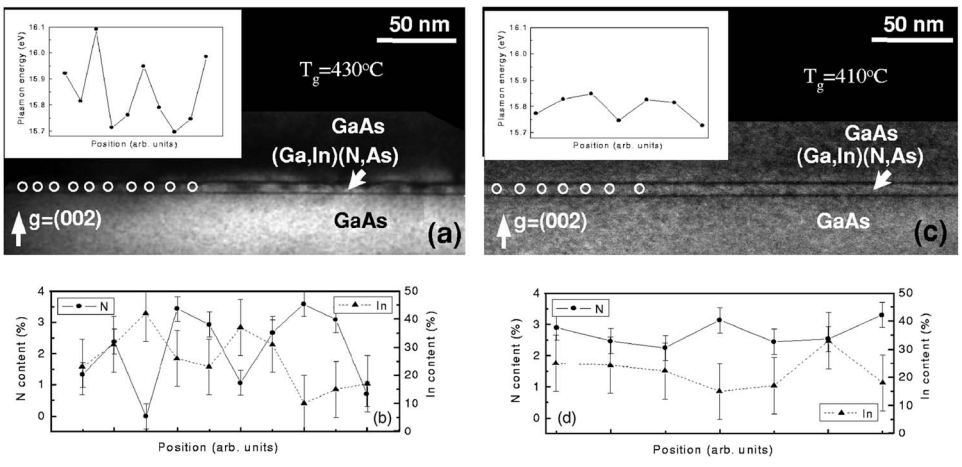

FIG. 2. Cross-sectional (002) dark-field TEM images of (Ga,In)(N,As) QW grown at 430 °C (a) and 410 °C (c). Scans of low-loss EEL spectra along both QWs are marked by circles, the corresponding plasmon energies are given in the insets. The results of the N and In contents are summarized in (b) and (d), respectively.

appears in uniform contrast with smooth interfaces. In order to analyze the element distribution along the QWs, an electron beam is generated with about 8 nm spot size, which is smaller than the periodicity of the measured contrast modulation. A scan of low-loss EEL spectra along the QWs is performed as indicated by the row of circles in Fig. 2(a). The appropriate plasmon energies shown in the inset of Fig. 2(a) indicate the inhomogeneous lateral distribution of N atoms. The maximal variation in E_p amounts to 0.4 eV describing a fluctuation of the N content between 0% and 3.5%. The corresponding In content varies at these positions between 10% and 42%. All results of the local In and N distribution along the QW are summarized in Fig. 2(b). The curves, which reflect the lateral element distributions, show a periodic oscillation similar to the contrast modulation in the dark-field TEM. However, both curves follow an opposite trend, i.e., positions with high N content correspond to low In concentration and vice versa. Therefore, the contrast modulation seen in Fig. 2(a) is not only the result of fluctuations in the N but also in the In composition. This finding indicates that there are regions along the QW with preferred formation of Ga–N and In–As bond configurations, respectively, although this structure leads to a higher local strain. On the other hand, the EEL spectroscopy of the QW grown at lower temperature (410 °C), where uniform contrast and smooth interfaces are observed in the (002) dark-field image [Fig. 2(c)], indicates almost no composition fluctuations for both elements [see Fig. 2(d)].

The ideal element distribution in a quaternary alloy, i.e., its nearest-neighbor bond configuration, is determined by minimizing the alloy free energy, which includes local strain and cohesive bond energy terms. The local strain is produced by the differences in bond lengths between the corresponding III–V atom combinations.[21] During the epitaxial growth, the physisorbed adatoms are able to relieve local strain toward the free surface. Therefore, the development of nearest-neighbor configurations is more driven by maximizing the cohesive bond energy than minimizing the local strain. Taking into account the values for the cohesive energies of the various bond configurations (for GaN, InN, GaAs, and InAs, being 2.24, 1.93, 1.63, and 1.55 eV/bond, respectively[22]), the formation of Ga–N and In–As bonds should be favored inducing an inherent composition modulation near the growing surface. Lowering the growth temperature results in a reduction of the adatom mobilities, which is responsible for a lower probability to generate the favorable bonds. The composition modulation is hence suppressed, in agreement with our observation [Fig. 2(d)]. On the other hand, this inherent composition modulation is associated with a strong increase of the epitaxial strain energy. Areas with preferred Ga–N and In–As bonds cause a higher epitaxial strain to the GaAs substrate compared to the case of Ga–As and In–N (for GaN, InN, GaAs, and InAs, being 1.94, 2.15, 2.45, and 2.61 Å, respectively[22]). Therefore, elastic strain energy is accumulated during growth until surface roughening starts that finally initiates a two-dimensional (2D) to three-dimensional (3D) growth mode transition.[8]

In conclusion, we have investigated the local element distribution in as-grown (Ga,In)(N,As) quantum wells grown on GaAs (001) substrates using low-loss EEL spectroscopy in combination with dark-field TEM. Distinct lateral fluctuations of the N and In concentrations were observed in the $Ga_{0.7}In_{0.3}N_{0.03}As_{0.97}$ QW grown at 430 °C following an opposite trend and indicating preferred Ga–N and In–As bond configurations. This phase decomposition is explained by the strong influence of the cohesive bond energy on the development of the nearest-neighbor arrangement on the growing surface.

This work was financially supported by the IST program of European Commission, Project No. IST-2000-26478-GINA1.5.

[1] M. Kondow, K. Uomi, A. Niwa, T. Kitatani, S. Watahiki, and Y. Yazawa, Jpn. J. Appl. Phys., Part 1 **35**, 1273 (1996).
[2] I. Ho and G. B. Stringfellow, J. Cryst. Growth **178**, 1 (1997).
[3] J. Neugebauer and C. Van de Walle, Phys. Rev. B **51**, 10568 (1995).
[4] H. P. Xin and C. W. Tu, Appl. Phys. Lett. **72**, 2442 (1998); A. Kaschner, T. Lüttgert, H. Born, A. Hoffmann, A. Yu. Egorov, and H. Riechert, *ibid.* **78**, 1391 (2001).
[5] W. Li, M. Pessa, T. Ahlgren, and J. Decker, Appl. Phys. Lett. **79**, 1094 (2001); Z. Pan, L. H. Li, W. Zhang, Y. W. Lin, R. H. Wu, and W. Ge, *ibid.* **77**, 1280 (2000); S. Kurtz, J. Webb, L. Gedvilas, D. Friedmen, J. Geisz, J. Olson, R. King, D. Joslin, and N. Karam, *ibid.* **78**, 748 (2001).
[6] S. Kurtz, J. Webb, L. Gedvilas, D. Friedman, J. Geisz, J. Olson, R. King, D. Joslin, and N. Karam, Appl. Phys. Lett. **78**, 748 (2001); P. J. Klar, H. Grüning, J. Koch, S. Schaefer, K. Volz, W. Stolz, W. Heimbrodt, A. M. K. Saadi, A. Lindsay, and E. P. O'Reilly, Phys. Rev. B **64**, 121203 (2001); V. Lordi, V. Gambin, S. Friedrich, T. Funk, T. Akizawa, K. Uno, and J. S. Harris, Phys. Rev. Lett. **90**, 145505 (2003).
[7] J.-M. Chauveau, A. Trampert, M.-A. Pinault, E. Tournié, and K. H. Ploog, Appl. Phys. Lett. **82**, 3451 (2003).
[8] A. Trampert, J.-M. Chauveau, K. H. Ploog, E. Tournié, and A. Guzmán, J. Vac. Sci. Technol. B **22**, 2195 (2004).
[9] H. P. Xin, K. L. Kavanagh, Z. Q. Zhu, and C. W. Tu, J. Vac. Sci. Technol. B **17**, 1649 (1999); H. P. Xin, K. L. Kavanagh, M. Kondow, and C. W. Tu, J. Cryst. Growth **201/202**, 419 (1999).
[10] A. Gutiérrez-Sosa, U. Bangert, A. Harvey, C. J. Fall, R. Jones, P. R. Briddon, and M. I. Heggie, Phys. Rev. B **66**, 035302 (2002).
[11] V. J. Keast, A. J. Scott, M. J. Kappers, C. T. Foxon, and C. J. Humphreys, Phys. Rev. B **66**, 125319 (2002).
[12] M. H. Gass, A. J. Papworth, T. B. Joyce, T. J. Bullough, and P. R. Chalker, Appl. Phys. Lett. **84**, 1453 (2004); M. H. Gass, A. J. Papworth, T. J. Bullough, and P. R. Chalker, Ultramicroscopy **101**, 257 (2004).
[13] E. Tournié, M.-A. Pinault, M. Laügt, J.-M. Chauveau, A. Trampert, and K. H. Ploog, Appl. Phys. Lett. **82**, 1845 (2003).
[14] R. F. Egerton, *Electron Energy Loss Spectroscopy in the Electron Microscope*, 2nd ed. (Plenum, New York, 1996).
[15] J. N. Chapman, J. D. Steele, J. H. Paterson, and J. M. Titchmarsh, Inst. Phys. Conf. Ser. **78**, 177 (1985).
[16] H. M. Chan and D. B. Williams, Philos. Mag. B **52**, 1019 (1985).
[17] P. J. Thomas and P. A. Midgley, Ultramicroscopy **88**, 179 (2001).
[18] The systemic error coming from the background removing and hydrocarbon contamination was estimated from substrate GaAs.
[19] In order to reduce the experimental errors, the zero energy is determined by fitting Gaussian function to zero-loss peak and the E_p is by accurate fitting the single scattering spectra within 11–18 eV with the Drude function (Ref. 14), which contain main part of plasmon excitation and decrease the influence of In 4*d* and Ga 3*d* transitions.
[20] I. Vurgaftman, J. R. Meyer, and L. R. Ram-Mohan, J. Appl. Phys. **89**, 5815 (2001); **94**, 3675 (2003), and references therein.
[21] K. Kim and A. Zunger, Phys. Rev. Lett. **86**, 2609 (2001).
[22] W. A. Harrison, *Electronic Structure and the Properties of Solids* (Dover, New York, 1989), pp. 175–176.